

Nonlinear Interferometry for Quantum-Enhanced Measurements of Multiphoton Absorption

Shahram Panahiyan^{1,2,3,*}, Carlos Sánchez Muñoz⁴, Maria V. Chekhova^{5,6} and Frank Schlawin^{1,2,3,†}

¹Max Planck Institute for the Structure and Dynamics of Matter, Luruper Chaussee 149, 22761 Hamburg, Germany

²The Hamburg Centre for Ultrafast Imaging, Luruper Chaussee 149, Hamburg D-22761, Germany

³University of Hamburg, Luruper Chaussee 149, 22761 Hamburg, Germany

⁴Departamento de Física Teórica de la Materia Condensada and Condensed Matter Physics Center (IFIMAC), Universidad Autónoma de Madrid, 28049 Madrid, Spain

⁵Max-Planck Institute for the Science of Light, Staudtstraße 2, Erlangen D-91058, Germany

⁶University of Erlangen-Nuremberg, Staudtstraße 7/B2, Erlangen D-91058, Germany



(Received 6 October 2022; revised 30 March 2023; accepted 25 April 2023; published 19 May 2023)

Multiphoton absorption is of vital importance in many spectroscopic, microscopic, or lithographic applications. However, given that it is an inherently weak process, the detection of multiphoton absorption signals typically requires large field intensities, hindering its applicability in many practical situations. In this Letter, we show that placing a multiphoton absorbent inside an imbalanced nonlinear interferometer can enhance the precision of multiphoton cross section estimation with respect to strategies based on photon-number measurements using coherent or even squeezed light directly transmitted through the medium. In particular, the power scaling of the sensitivity with photon flux can be increased by 1 order compared with transmission measurements of the sample with coherent light, such that the measurement precision at any given intensity can be greatly enhanced. Furthermore, we show that this enhanced measurement precision is robust against experimental imperfections leading to photon losses, which usually tend to degrade the detection sensitivity. We trace the origin of this enhancement to an optimal degree of squeezing which has to be generated in a nonlinear SU(1,1) interferometer.

DOI: [10.1103/PhysRevLett.130.203604](https://doi.org/10.1103/PhysRevLett.130.203604)

Introduction.—Multiphoton absorption (MPA) is a nonlinear process in which several photons are simultaneously absorbed by the sample [1–3]. Large penetration depths and the nonlinear dependence on the beam profile, causing most of the signal to be generated in the confined area of maximal beam intensity, make it an appealing process for a variety of technological applications. Most famously, in nonlinear imaging, multiphoton processes can surpass the single-photon diffraction limit and thereby enhance the spatial resolution [4–6], pushing the resolution of optical microscopy to molecular scales. Two-photon absorption (i.e., $m = 2$) already forms the foundation for diverse applications ranging from 3D microfabrication [7] to optical data storage [8], spectroscopy, and microscopy [9–11] and even medical applications such as photodynamic therapy [12]. Furthermore, processes with $m \geq 3$ have been explored for photon absorption microscopy due to a reduction of scattering losses and further minimization of unwanted linear

absorption. They provide greater penetration depth and spatial resolution [13], making them ideal tools for inorganic-organic hybrid materials [10] and biological imaging [14–19].

These advantages offered by MPA are, however, limited by the inherent weakness of nonlinear light-matter interactions [20,21] and the resulting very small multiphoton absorption cross sections, such that typically the use of strong, ultrafast lasers is the only way to overcome this problem and generate a measurable signal.

One way to circumvent the low efficiency of such interactions may lie in the exploitation of the quantum properties of light [22]. In particular, two-photon absorption of nonclassical light has attracted tremendous interest in this regard [23–31], where enhanced nonlinear signals induced by entangled photons were reported [30]. The strength of this enhancement is, however, the subject of intense current debate [32–37]. Moreover, even if large enhancements due to entanglement were feasible, because of its occurrence in the few-photon regime, where the mean photon number per mode must be small, $\langle \hat{n} \rangle \lesssim 1$, it is not suitable for many practical applications, such as nonlinear imaging, where a nonlinear photon flux dependence, which requires $\langle \hat{n} \rangle \gg 1$, is crucial to enhance the resolution.

Published by the American Physical Society under the terms of the [Creative Commons Attribution 4.0 International](https://creativecommons.org/licenses/by/4.0/) license. Further distribution of this work must maintain attribution to the author(s) and the published article's title, journal citation, and DOI. Open access publication funded by the Max Planck Society.

This motivates us to investigate, more broadly, MPA of nonclassical states of light with mesoscopic character, i.e., with large photon numbers compared with entangled photon sources. With notable exceptions [38,39], this photon number regime has received much less attention in the literature to date, even though it is very attractive for said applications. The rate of m -photon absorption scales with the m th order correlation function, which, for bunched sources, grows exponentially with m [40]. But for practical applications, this enhancement has to be compared with the increased noise levels of these sources which may erode the benefits. We investigated two-photon absorption recently [41,42], and found improved scaling behavior of the Fisher information in quadrature measurements with displaced squeezed light compared with coherent states of light. However, the question remains: how to find a realistic setup to perform this quantum-enhanced nonlinear spectroscopy?

One particularly promising platform for investigating the nonlinear interactions of bright quantum states of light is nonlinear SU(1,1) interferometers [43–45]. Introduced theoretically by Yurke already in the 1980s [46], this technology has reached a level of maturity where various applications in quantum sensing seem feasible. It can be used, *inter alia*, for phase measurements [47], spectroscopy [48,49], imaging [50], quantum state engineering [51,52], and quantum information applications [53,54]. The main difference between these nonlinear interferometers and their linear Mach-Zehnder counterparts is the replacement of the beam splitters with optical parametric amplifiers (OPA) [45]. In the single-mode case considered in this manuscript, these OPAs squeeze (or antisqueeze) a field quadrature of the light field propagating through the setup, and can thereby enhance resolution or suppress the impact of certain noise sources. It is known that the second OPA renders phase measurements robust against single-photon losses that occur outside the interferometer [47,50,55–61]. Recently, the same improvement was also predicted in linear absorption measurements in the low-gain regime [60]. However, to the best of our knowledge, multiphoton absorption measurements have not been investigated to date in this platform.

In this Letter, we will show that by placing an MPA sample inside a nonlinear SU(1,1) interferometer [43] and optimizing the interferometer, the resolution of a MPA signal can be enhanced significantly compared with MPA detection using a classical source with the same photon number. In particular, while the uncertainty $\Delta\varepsilon_m^2$ for measurements of the m -photon absorbance ε_m with classical light scales as $\sim n_S^{-2m+1}$ for sufficiently large photon numbers (n_S) at the sample, we find that this scaling can be enhanced to n_S^{-2m} in a nonlinear SU(1,1) interferometer, thus providing an enormous advantage in the large photon number regime considered here. We find a set of parameters of the interferometer that optimize the

measurable $\Delta\varepsilon_m^2$, and we characterize the resulting light fields. This analysis enables us to identify parameter regimes where nonlinear interferometers can detect MPA signals, but which are inaccessible with classical methods. In addition, we explore the effects of error sources (in the literature referred to as internal and external losses [56–58]) on the MPA detection ability. Crucially, we find that so-called external losses do not degrade the sensitivity of the measurements, as they can be compensated in nonlinear interferometers. As is also the case in phase estimation [45], however, so-called internal losses cannot be compensated, and reduce the optimal achievable precision scaling.

Setup and theory.—The setup we consider in this Letter is sketched in Fig. 1(a): a coherent seed field with central frequency ω_0 is injected into a degenerate OPA, where a pump pulse with central frequency $2\omega_0$ triggers stimulated single-mode downconversion and creates a squeezed coherent state that interacts with an m -photon absorbing sample [62,63]. It should be noted that in most experiments on downconversion driven by pulsed pump fields, multimode states of light are created. In order to generate single-mode squeezed light, one should enforce single-mode spontaneous parametric downconversion (SPDC) with specially chosen phase matching [64] via methods such as dispersion engineering [65], parametric amplification after group-velocity dispersion [51], or using waveguides [63,66]. We account for scattering losses in the optical system after MPA (internal losses), which we characterize by the loss rate $1 - \eta_{\text{In}}$ ($\eta_{\text{In}} = 1$ corresponds to no loss while $\eta_{\text{In}} = 0$ indicates all the photons are completely lost). Single-photon losses occurring inside the sample are discussed in the Supplemental Material [67]. The transmitted light field passes through the second OPA where it will be squeezed or antisqueezed. Finally, the light field reaches the detector, where an intensity measurement is carried out. We account for imperfect photon detection with a second loss process (the so-called external losses), described by the loss rate $1 - \eta_{\text{Ex}}$. Taken together, the expectation value of the photon number measurement after the transmission through the described setup can be calculated as

$$\langle \hat{n} \rangle = \text{tr} \{ \hat{n} e^{\mathcal{L}_{\text{loss}2}} e^{\mathcal{L}_{\text{OPA}2}} e^{\mathcal{L}_{\text{loss}1}} e^{\mathcal{L}_{\text{MPA}\varepsilon_m}} e^{\mathcal{L}_{\text{OPA}1}} \rho_0 \}. \quad (1)$$

Here, $\rho_0 = \mathcal{D}(\alpha)|0\rangle\langle 0|\mathcal{D}^\dagger(\alpha)$ describes the initial coherent seed state with the complex displacement amplitude $\alpha = |\alpha|e^{i\phi_{\text{Las}}}$, in which “Las” stands for laser. $\mathcal{L}_{\text{OPA}k}$ are superoperators describing the squeezing processes,

$$e^{\mathcal{L}_{\text{OPA}k}} \rho \equiv U_{\text{OPA}k} \rho U_{\text{OPA}k}^\dagger, \quad (2)$$

where $U_{\text{OPA}k} = \exp(\zeta_k a^\dagger{}^2/2 - \zeta_k^* a^2/2)$ and $\zeta_k = r_k e^{i\phi_k}$. Without loss of generality, we set the phase of the first OPA as $\phi_1 = 0$ and rename the phase of the second OPA as $\phi_2 = \phi_{\text{Int}}$ (where “Int” stands for the interferometer).

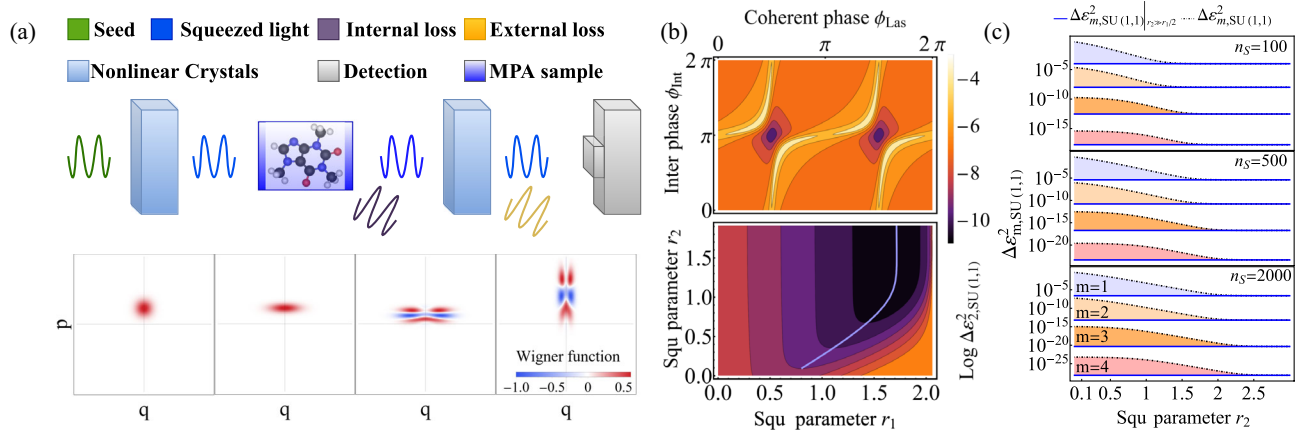


FIG. 1. (a) The setup considered in this manuscript. A coherent seed pulse passes through a first degenerate OPA on the left which prepares a squeezed state. It is focused on an m -photon absorption sample, where a part of the light field is lost due to single-photon scattering. The transmitted light field is then focused on a second degenerate OPA. The light field finally reaches the detection device on the right where imperfect detection gives rise to another loss source. (b) Variance $\Delta \epsilon_{m, \text{SU}(1,1)}^2$ for two-photon absorption ($m = 2$) with $\eta_{\text{In}} = \eta_{\text{Ex}} = 1$, and $n_S = 15$, as a function of interferometer and laser phases (upper panel with $r_1 = 0.939$ and $r_2 = 1.447$) and also as a function of squeezing parameters (lower panel with $\phi_{\text{Las}} = \pi/2$ and $\phi_{\text{Int}} = \pi$). The sensitivity becomes independent of the second squeezing parameter for a sufficiently large second squeezing parameter r_2 . The light blue line maps optimal regimes of squeezing parameters. (c) $\Delta \epsilon_{m, \text{SU}(1,1)}^2$ (dotted-dashed lines) and Eq. (7) (solid lines) as a function of second squeezing parameter for different photon numbers at the sample (n_S). We observe that for sufficiently large second squeezing parameter r_2 , $\Delta \epsilon_{m, \text{SU}(1,1)}^2$ converges to the scaling behavior reported in Eq. (7) (for sufficiently high n_S).

$\mathcal{L}_{\text{loss } k}$ account for single-photon losses which we model as unbalanced beam splitters [47,68–70], i.e.,

$$e^{\mathcal{L}_{\text{loss } k}} \rho = U_{\text{loss } k} \rho U_{\text{loss } k}^\dagger, \quad (3)$$

in which $U_{\text{loss } k} = \exp(\tau_k(ac_k^\dagger + c_k a^\dagger/2))$, with $\tau_k = \arccos(\sqrt{\eta_k})$, and c_k is a photon annihilation operator in an auxiliary mode that remains in a vacuum state. Finally, the dynamics of the transmission of a quantum state of light through an m -photon absorbing medium is described by a Markovian Lindblad master equation for the photonic density matrix ρ in a reference frame rotating at the frequency ω_0 [71,72]

$$\frac{d}{dt} \rho = \gamma_{\text{MPA}} \mathcal{L}_{\text{MPA}} \rho = \frac{\gamma_{\text{MPA}}}{2m} (2a^m \rho a^{\dagger m} - a^{\dagger m} a^m \rho - \rho a^{\dagger m} a^m). \quad (4)$$

The Lindblad operator is given by a correlated loss operator $L = a^m/\sqrt{m}$. We add the factor m in the definition of the Lindblad operator for convenience to simplify expressions in our subsequent derivations. Given the time t in which the light field travels through the sample, we wish to estimate the absorbance $\epsilon_m \equiv \gamma_{\text{MPA}} t$ which can be related to the corresponding m -photon absorption cross section (see the Supplemental Material [67]). The precision of estimating ϵ_m can be obtained by studying the uncertainty of ϵ_m via error

propagation [73,74], yielding the following expression for the variance of intensity measurements

$$\Delta \epsilon_m^2 = \frac{\text{Var}(\hat{n})}{\left| \frac{\partial \langle \hat{n} \rangle}{\partial \epsilon_m} \right|^2}. \quad (5)$$

The variance $\Delta \epsilon_m^2$ determines the smallest absorbance ϵ_m that can be distinguished from a zero signal and consequently, the improvement of its scaling behavior provides an enormous advantage in practical applications where the photon flux should be kept as small as possible. Since nonlinear susceptibilities, and hence the corresponding multiphoton absorption cross sections, decline rapidly with m (see the Supplemental Material [67]), we concentrate on the weak absorption limit, where $\epsilon_m \ll 1$. Consequently, we will approximate $e^{\mathcal{L}_{\text{MPA}} \epsilon_m} \simeq \mathbb{1} + \epsilon_m \mathcal{L}_{\text{MPA}}$ which results in the transmitted density matrix being $\rho' \simeq \rho + \epsilon_m (\partial \rho / \partial \epsilon_m)$.

Let us first consider a conventional transmission measurement of MPA losses using a strong laser with $\langle \hat{n} \rangle \gg 1$. The precision can be found straightforwardly from Eqs. (1) and (5) by setting $r_1 = r_2 = 0$. It evaluates to

$$\Delta \epsilon_{m, (\text{coh})}^2 = \frac{1}{\eta_{\text{In}} \eta_{\text{Ex}}} \frac{1}{n_S^{2m-1}}, \quad (6)$$

where n_S (the number of photons at the sample) in Eq. (6) is simply $n_S = |\alpha|^2$. This behavior originates from the

m -photon absorption signal scaling $\propto n_S^m$ and the variance of the intensity (hence, the photon number) increasing linearly for a coherent state. Altogether, the precision scales as the $(2m - 1)$ -th power of the mean photon number, and it is reduced by both internal and external losses. As we show in what follows, an interferometric detection can reduce the photon number variance to a constant, without deteriorating the signal scaling.

Interferometric enhancement.—We now want to understand how the SU(1,1) interferometer can enhance the resolution of MPA measurements compared with Eq. (6). To this end, we first establish conditions for optimizing the sensitivity, i.e., for minimizing the variance [Eq. (5)]. Since the photon number in the interferometer can vary strongly with, e.g., the phases ϕ_i , we fix the number of photons at the sample (n_S) in the optimization procedure. This requirement is inspired by the central objective in quantum-enhanced sensing applications to reduce photodamage at the sample. Instead, we allow for a varying number of photons at the detector level, where photodamage is not problematic. As a consequence, the first squeezing parameter is bounded within $0 \leq r_1 \leq \text{arcsinh} \sqrt{n_S}$, and the coherent amplitude $|\alpha|$ is adjusted to keep the photon number at the sample fixed resulting in $n_S = |\alpha|^2 [\sinh(2r_1) \cos(2\phi_{\text{Las}}) + \cosh(2r_1)] + \frac{1}{2} [\cosh(2r_1) - 1]$. Thus, $r_1 = \text{arcsinh} \sqrt{n_S}$ will correspond to a squeezed vacuum (and also $|\alpha| = 0$), while $r_1 = 0$ corresponds to a coherent state with $|\alpha| = \sqrt{n_S}$ propagating through the sample.

In Fig. 1(b), we present the parameter optimization for $m = 2$ at a fixed photon number $n_S = 15$ showing that we obtain the best precision when the phases are fixed at $\phi_{\text{Las}} = \pi/2, 3\pi/2, \dots$ and $\phi_{\text{int}} = \pi$. This result does not change for $m = 1, \dots, 4$ [75] and does not depend on the photon number n_S . It can be interpreted as illustrated in the small panels in Fig. 1(a): The first condition implies that the first OPA generates an amplitude-squeezed state (here by squeezing the momentum quadrature). This photon-number-squeezing enables the phase-insensitive multiphoton loss to create the strongest possible signal by changing its sub-Poissonian photon number distribution. We recently showed that such a state is well suited to detect two-photon losses [42], and this remains true for general m -photon absorption. The second condition above, $\phi_{\text{int}} = \pi$, implies that the second OPA antisqueezes the initially squeezed quadrature, which means that the sub-Poissonian distribution is stretched into a super-Poissonian one thus enhancing the change brought about by the MPA. This is illustrated in the third and fourth small panels in Fig. 1(a).

The optimal choice of phases has to be accompanied by a suitable degree of squeezing. This is depicted in Fig. 1(b), where we minimize Eq. (5) as a function of both squeezing parameters r_1 and r_2 . For any fixed r_2 , there is a minimum as a function of r_1 . This means that the optimal sensitivity is generated by an amplitude-squeezed state, where the amount of squeezing has to be adjusted for the mean photon

number n_S , as we will discuss later in detail. In addition, the optimal squeezing r_1 increases with r_2 and then saturates [see Fig. 1(c)], as does the achievable precision at fixed n_S . This demonstrates that the interferometer can enhance the precision of MPA detection.

If we optimize r_1 at every n_S we find that if, in the absence of external losses, $r_2 \gg r_1/2$ (for details, see the Supplemental Material [67]), Eq. (5) scales as

$$\Delta \varepsilon_{m, \text{SU}(1,1)}^2 |_{r_2 \gg r_1/2} \propto \frac{1}{n_S^{2m}} \quad (7)$$

for sufficiently large n_S . This scaling is contrasted with the classical case [Eq. (6)] in Fig. 2(a) for $m = 1, \dots, 4$. Thus, the optimal choice of parameters enables us to increase the scaling of the sensitivity with respect to the mean photon number by a factor of 1. This is the central result of our paper.

Impact of losses.—We next investigate how the quantum-enhanced sensitivity scaling is affected by the inevitable photon losses in a realistic experiment. We first note that in the limit of large r_2 considered before, Eq. (5) becomes independent of external losses (see the Supplemental Material [67]). This is again consistent with our earlier results [42], where it was shown that single-photon losses do not affect the sensitivity of two-photon absorption measurements with squeezed states. Hence, external losses can always be compensated in an SU(1,1) interferometer [51,56]. This behavior contrasts with the classical situation in Eq. (6), where the resolution is degraded by external losses. This behavior is shown in Fig. 2(b). While we can have sensitivity advantages for $r_1/2 < r_2 < r_1$, in order to remove the effects of the external loss completely and saturate the optimum scaling behavior as we have described above, we should further demand $r_1 < r_2$, such that we generate super-Poissonian photon statistics at the detector.

The same is not true for internal losses. If these losses destroy squeezing in the light field before it reaches the second OPA, the quantum advantage we obtained in Eq. (7) is lost. This behavior is shown in Fig. 2(c), where we extract the scaling behavior of $\Delta \varepsilon_m^2$ (i.e., we determine the scaling $\Delta \varepsilon_m^2 \sim n_S^{-\gamma}$ for $n_S > 100$) as a function of these internal losses. At small internal losses ($1 - \eta_{\text{in}} \lesssim 10^{-3}$), the scaling is not affected, and we find $\gamma \sim 2m$. The scaling exponent then decreases gradually and approaches the coherent limit $\gamma \sim 2m - 1$ when the internal losses become very large ($1 - \eta_{\text{in}} \sim 0.1$) [47,54]. It should be noted that although the scaling behavior of the coherent case is not affected by internal loss, the optimum sensitivity would be affected similarly to the external case [see Eq. (6)]. There is a quantum enhancement (albeit a small one) even for strong internal losses of, say, 10%. Remarkably, overall our findings appear analogous to linear phase estimation applications, where internal losses destroy the sought-after

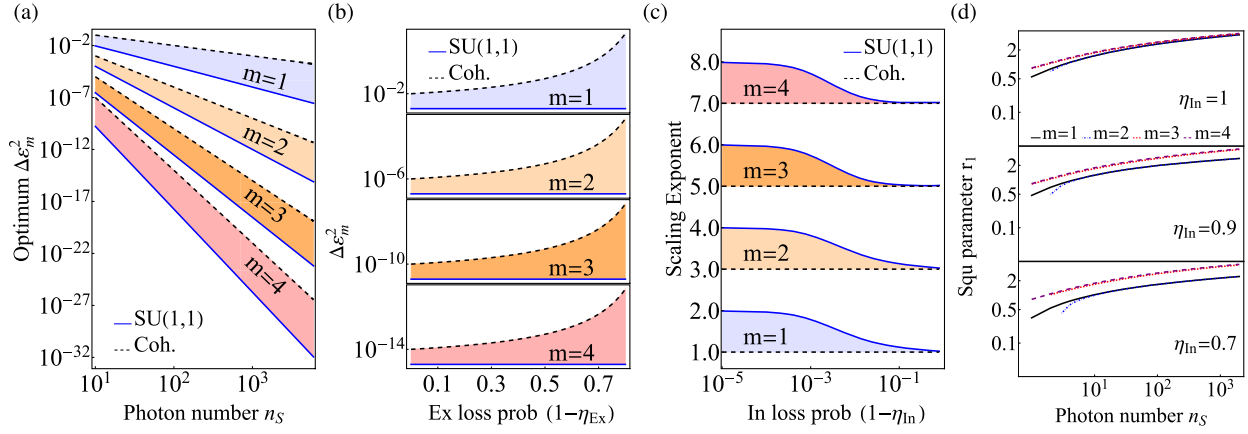


FIG. 2. (a) Optimum $\Delta\epsilon_m^2$ as a function of the photon number interacting with the sample, n_S . We observe that squeezing inside the SU(1,1) interferometer enhances the best achievable sensitivity compared with a classical interferometer. (b) Eq. (5) is shown in the limit of very large r_2 as a function of external losses for optimized SU(1,1) measurements (solid lines) and coherent states (dashed lines) in the case of one-, two-, three-, and four-photon absorption. By adjusting the squeezing parameters, the effects of external loss can be completely compensated in the SU(1,1) case. (c) Scaling exponent γ of the sensitivity (i.e., $\Delta\epsilon_m^2 \sim n_S^{-\gamma}$) as a function of the internal loss. SU(1,1) interferometric measurements show superior precision scaling compared with coherent state measurements even in the presence of strong internal loss, up to $\sim 10\%$. (d) The optimal squeezing parameter r_1 as a function of photon number for three different levels of internal loss. Overall, we observe that higher-order nonlinear processes have better sensitivity indicating that the measurement of the cross section in samples with higher-order nonlinear processes has better precision.

Heisenberg scaling, while external losses can be compensated [47,50,55–59].

Optimal squeezing parameter.—We finally turn to the discussion of the optimal squeezed state in the interferometer. The observed enhancement is a consequence of the optimal squeezing or antisqueezing operations performed by the two OPAs. While the second squeezing parameter should be chosen as large as possible, the first squeezing parameter is determined by three factors: the number of photons n_S , the internal loss $1 - \eta_{In}$, and the degree of the nonlinearity m . We show its variation with n_S in Fig. 2(d). In an ideal interferometer, $\eta_{In} = 1$, the first OPA generates an amplitude-squeezed state [see Fig. 1(a)] where the standard deviation of the antisqueezed quadrature is as large as the expectation value of the squeezed one, i.e., $\langle q^2 \rangle^{1/2} = \langle p \rangle$. As we show in the Supplemental Material [67], this condition gives rise to the enhanced scaling in Eq. (7), by keeping the variance in the numerator of Eq. (5) constant, while admitting an optimal scaling of the denominator. This optimal degree of squeezing decreases with the internal loss in the case of one- and two-photon absorption but remains almost constant for larger nonlinearities. Thus, the condition $\langle q^2 \rangle^{1/2} = \langle p \rangle$ appears to describe an almost universally optimal state for detecting multiphoton absorption.

Conclusion.—We found that at any given intensity of light interacting with the sample, SU(1,1) interferometers can improve significantly the precision of estimation of multiphoton absorbances with respect to approaches based on classical light. At photon fluxes with mean photon number $\langle \hat{n} \rangle > 1$, the precision of an optimally tuned

SU(1,1) interferometer scales as $\sim n_S^{-2m}$. In contrast, a classical measurement only realizes a scaling $\sim n_S^{-2m+1}$. A measurement with the optimized ideal SU(1,1) interferometer can thus always outperform its classical counterpart. Even in the presence of competing losses, optimized quantum states always outperform classical measurement strategies. We note that this performance is also superior to transmission measurements with squeezed light (see Ref. [42]). While we concentrated on multiphoton absorption, a similar SU(1,1) interferometer provides interesting quantum enhancements for other nonlinear spectroscopic processes such as Raman signals [48]. The generalization to multimode interferometers will be another important avenue to explore, as it will enable the exploitation of entanglement to create further metrological and spectroscopic advantages in nonlinear interferometry [76–79]. Our work establishes a quantum advantage for high-gain squeezed light that opens new applications in quantum imaging [80,81] in a nonlinear intensity regime.

S. P. and F. S. acknowledge support from the Cluster of Excellence “Advanced Imaging of Matter” of the Deutsche Forschungsgemeinschaft (DFG)—EXC 2056—Project ID No. 390715994. C. S. M. acknowledges that the project that gave rise to these results received the support of a fellowship from la Caixa Foundation (ID No. 100010434) and from the European Union Horizon 2020 research and innovation program under the Marie Skłodowska-Curie Grant Agreement No. 847648, with fellowship code LCF/BQ/PI20/11760026, and financial support from the Proyecto Sinérgico CAM 2020 Y2020/TCS-6545

(NanoQuCo-CM). M. V. C. acknowledges support from QuantERA II Programme (project SPARQL) which has received funding from the European Union's Horizon 2020 research and innovation program under Grant Agreement No. 101017733, with the funding organization Deutsche Forschungsgemeinschaft.

*shahram.panahiyan@mpsd.mpg.de

†frank.schlawin@mpsd.mpg.de

- [1] P. Cronstrand, Y. Luo, and H. Ågren, Multi-photon absorption of molecules, in *Advances in Quantum Chemistry, Response Theory and Molecular Properties (A Tribute to Jan Lindberg and Poul Jørgensen)* (Academic Press, New York, 2005), Vol. 50, pp. 1–21.
- [2] F. Dell'Anno, S. De Siena, and F. Illuminati, Multiphoton quantum optics and quantum state engineering, *Phys. Rep.* **428**, 53 (2006).
- [3] M. Rumi and J. W. Perry, Two-photon absorption: An overview of measurements and principles, *Adv. Opt. Photonics* **2**, 451 (2010).
- [4] T. A. Klar, S. Jakobs, M. Dyba, A. Egner, and S. W. Hell, Fluorescence microscopy with diffraction resolution barrier broken by stimulated emission, *Proc. Natl. Acad. Sci. U.S.A.* **97**, 8206 (2000).
- [5] S. Bretschneider, C. Eggeling, and S. W. Hell, Breaking the Diffraction Barrier in Fluorescence Microscopy by Optical Shelving, *Phys. Rev. Lett.* **98**, 218103 (2007).
- [6] P. T. C. So, C. Y. Dong, B. R. Masters, and K. M. Berland, Two-photon excitation fluorescence microscopy, *Annu. Rev. Biomed. Eng.* **2**, 399 (2000).
- [7] H.-B. Sun, T. Kawakami, Y. Xu, J.-Y. Ye, S. Matuso, H. Misawa, M. Miwa, and R. Kaneko, Real three-dimensional microstructures fabricated by photopolymerization of resins through two-photon absorption, *Opt. Lett.* **25**, 1110 (2000).
- [8] P. D. A. and R. P. M., Three-dimensional optical storage memory, *Science* **245**, 843 (1989).
- [9] F. Helmchen and W. Denk, Deep tissue two-photon microscopy, *Nat. Methods* **2**, 932 (2005).
- [10] S. J. Weishäupl, D. C. Mayer, Y. Cui, P. Kumar, H. Oberhofer, R. A. Fischer, J. Hauer, and A. Pöthig, Recent advances of multiphoton absorption in metal-organic frameworks, *J. Mater. Chem. C* **10**, 6912 (2022).
- [11] S. H. Lin, *Multiphoton Spectroscopy of Molecules* (Elsevier, New York, 2012).
- [12] M. Atif, P. E. Dyer, T. A. Paget, H. V. Snelling, and M. R. Stringer, Two-photon excitation studies of m-THPC photosensitizer and photodynamic activity in an epithelial cell line, *Photodiagn. Photodyn. Ther.* **4**, 106 (2007).
- [13] F. E. Hernández, K. D. Belfield, I. Cohanoschi, M. Balu, and K. J. Schafer, Three- and four-photon absorption of a multiphoton absorbing fluorescent probe, *Appl. Opt.* **43**, 5394 (2004).
- [14] D. Débarre, N. Olivier, W. Supatto, and E. Beaupaire, Mitigating phototoxicity during multiphoton microscopy of live drosophila embryos in the 1.0–1.2 μm wavelength range, *PLoS One* **9**, 1 (2014).
- [15] K. Toda, K. Isobe, K. Namiki, H. Kawano, A. Miyawaki, and K. Midorikawa, Temporal focusing microscopy using three-photon excitation fluorescence with a 92-fs yb-fiber chirped pulse amplifier, *Biomed. Opt. Express* **8**, 2796 (2017).
- [16] C. J. Rowlands, D. Park, O. T. Bruns, K. D. Piatkevich, D. Fukumura, R. K. Jain, M. G. Bawendi, E. S. Boyden, and P. T. So, Wide-field three-photon excitation in biological samples, *Light* **6**, e16255 (2017).
- [17] D. G. Ouzounov, T. Wang, M. Wang, D. D. Feng, N. G. Horton, J. C. Cruz-Hernández, Y.-T. Cheng, J. Reimer, A. S. Tolia, N. Nishimura, and C. Xu, In vivo three-photon imaging of activity of GCaMP6-labeled neurons deep in intact mouse brain, *Nat. Methods* **14**, 388 (2017).
- [18] B. Chen, X. Huang, D. Gou, J. Zeng, G. Chen, M. Pang, Y. Hu, Z. Zhao, Y. Zhang, Z. Zhou, H. Wu, H. Cheng, Z. Zhang, C. Xu, Y. Li, L. Chen, and A. Wang, Rapid volumetric imaging with bessel-beam three-photon microscopy, *Biomed. Opt. Express* **9**, 1992 (2018).
- [19] T. Wang, D. G. Ouzounov, C. Wu, N. G. Horton, B. Zhang, C.-H. Wu, Y. Zhang, M. J. Schnitzer, and C. Xu, Three-photon imaging of mouse brain structure and function through the intact skull, *Nat. Methods* **15**, 789 (2018).
- [20] B. R. Mollow, Two-photon absorption and field correlation functions, *Phys. Rev.* **175**, 1555 (1968).
- [21] R. W. Boyd, *Nonlinear Optics, Third Edition*, 3rd ed. (Academic Press, Inc., USA, 2008).
- [22] C. A. Casacio, L. S. Madsen, A. Terrasson, M. Waleed, K. Barnscheidt, B. Hage, M. A. Taylor, and W. P. Bowen, Quantum-enhanced nonlinear microscopy, *Nature* **594**, 201 (2021).
- [23] J. C. Matthews, X.-Q. Zhou, H. Cable, P. J. Shadbolt, D. J. Saunders, G. A. Durkin, G. J. Pryde, and J. L. O'Brien, Towards practical quantum metrology with photon counting, *npj Quantum Inf.* **2**, 16023 (2016).
- [24] K. E. Dorfman, F. Schlawin, and S. Mukamel, Nonlinear optical signals and spectroscopy with quantum light, *Rev. Mod. Phys.* **88**, 045008 (2016).
- [25] F. Schlawin, Entangled photon spectroscopy, *J. Phys. B* **50**, 203001 (2017).
- [26] J. P. Villabona-Monsalve, O. Calderón-Losada, M. Nuñez Portela, and A. Valencia, Entangled two photon absorption cross section on the 808 nm region for the common dyes zinc tetraphenylporphyrin and rhodamine b, *J. Phys. Chem. A* **121**, 7869 (2017).
- [27] F. Schlawin, K. E. Dorfman, and S. Mukamel, Entangled two-photon absorption spectroscopy, *Acc. Chem. Res.* **51**, 2207 (2018).
- [28] M. Gilaberte Basset, F. Setzpfandt, F. Steinlechner, E. Beckert, T. Pertsch, and M. Gräfe, Perspectives for applications of quantum imaging, *Laser Photonics Rev.* **13**, 1900097 (2019).
- [29] S. Szoke, H. Liu, B. P. Hickam, M. He, and S. K. Cushing, Entangled light-matter interactions and spectroscopy, *J. Mater. Chem. C* **8**, 10732 (2020).
- [30] A. Eshun, O. Varnavski, J. P. Villabona-Monsalve, R. K. Burdick, and T. Goodson, Entangled photon spectroscopy, *Acc. Chem. Res.* **55**, 991 (2022).
- [31] Y. Chen, R. d. J. León-Montiel, and L. Chen, Quantum interferometric two-photon excitation spectroscopy, *New J. Phys.* **24**, 113014 (2022).
- [32] M. G. Raymer, T. Landes, M. Allgaier, S. Merkouche, B. J. Smith, and A. H. Marcus, How large is the quantum

- enhancement of two-photon absorption by time-frequency entanglement of photon pairs?, *Optica* **8**, 757 (2021).
- [33] R. K. Burdick, G. C. Schatz, and T. Goodson, Enhancing entangled two-photon absorption for picosecond quantum spectroscopy, *J. Am. Chem. Soc.* **143**, 16930 (2021).
- [34] T. Landes, M. Allgaier, S. Merkouche, B. J. Smith, A. H. Marcus, and M. G. Raymer, Experimental feasibility of molecular two-photon absorption with isolated time-frequency-entangled photon pairs, *Phys. Rev. Res.* **3**, 033154 (2021).
- [35] T. Landes, M. G. Raymer, M. Allgaier, S. Merkouche, B. J. Smith, and A. H. Marcus, Quantifying the enhancement of two-photon absorption due to spectral-temporal entanglement, *Opt. Express* **29**, 20022 (2021).
- [36] K. M. Parzuchowski, A. Mikhaylov, M. D. Mazurek, R. N. Wilson, D. J. Lum, T. Gerrits, C. H. Camp, M. J. Stevens, and R. Jimenez, Setting Bounds on Entangled Two-Photon Absorption Cross Sections in Common Fluorophores, *Phys. Rev. Appl.* **15**, 044012 (2021).
- [37] B. P. Hickam, M. He, N. Harper, S. Szoke, and S. K. Cushing, Single-photon scattering can account for the discrepancies among entangled two-photon measurement techniques, *J. Phys. Chem. Lett.* **13**, 4934 (2022).
- [38] P. M. Birchall, E. J. Allen, T. M. Stace, J. L. O'Brien, J. C. F. Matthews, and H. Cable, Quantum Optical Metrology of Correlated Phase and Loss, *Phys. Rev. Lett.* **124**, 140501 (2020).
- [39] G. S. Atkinson, E. J. Allen, G. Ferranti, A. R. McMillan, and J. C. F. Matthews, Quantum Enhanced Precision Estimation of Transmission with Bright Squeezed Light, *Phys. Rev. Appl.* **16**, 044031 (2021).
- [40] K. Y. Spasibko, D. A. Kopylov, V. L. Krutyanskiy, T. V. Murzina, G. Leuchs, and M. V. Chekhova, Multiphoton Effects Enhanced Due to Ultrafast Photon-Number Fluctuations, *Phys. Rev. Lett.* **119**, 223603 (2017).
- [41] C. Sánchez Muñoz, G. Frascella, and F. Schlawin, Quantum metrology of two-photon absorption, *Phys. Rev. Res.* **3**, 033250 (2021).
- [42] S. Panahiyan, C. S. Muñoz, M. V. Chekhova, and F. Schlawin, Two-photon-absorption measurements in the presence of single-photon losses, *Phys. Rev. A* **106**, 043706 (2022).
- [43] M. V. Chekhova and Z. Y. Ou, Nonlinear interferometers in quantum optics, *Adv. Opt. Photonics* **8**, 104 (2016).
- [44] B. J. Lawrie, P. D. Lett, A. M. Marino, and R. C. Pooser, Quantum sensing with squeezed light, *ACS Photonics* **6**, 1307 (2019).
- [45] Z. Y. Ou and X. Li, Quantum Su(1,1) interferometers: Basic principles and applications, *APL Photonics* **5**, 080902 (2020).
- [46] B. Yurke, S. L. McCall, and J. R. Klauder, Su(2) and Su(1,1) interferometers, *Phys. Rev. A* **33**, 4033 (1986).
- [47] M. Manceau, G. Leuchs, F. Khalili, and M. Chekhova, Detection Loss Tolerant Supersensitive Phase Measurement with an Su(1,1) Interferometer, *Phys. Rev. Lett.* **119**, 223604 (2017).
- [48] Y. Michael, L. Bello, M. Rosenbluh, and A. Pe'er, Squeezing-enhanced Raman spectroscopy, *npj Quantum Inf.* **5**, 81 (2019).
- [49] K. E. Dorfman, Nonlinear interferometers with correlated photons: Toward spectroscopy and imaging with quantum light, *Light* **9**, 123 (2020).
- [50] G. Frascella, E. E. Mikhailov, N. Takanashi, R. V. Zakharov, O. V. Tikhonova, and M. V. Chekhova, Wide-field Su(1,1) interferometer, *Optica* **6**, 1233 (2019).
- [51] S. Lemieux, M. Manceau, P. R. Sharapova, O. V. Tikhonova, R. W. Boyd, G. Leuchs, and M. V. Chekhova, Engineering the Frequency Spectrum of Bright Squeezed Vacuum via Group Velocity Dispersion in an Su(1,1) Interferometer, *Phys. Rev. Lett.* **117**, 183601 (2016).
- [52] J. Su, L. Cui, J. Li, Y. Liu, X. Li, and Z. Y. Ou, Versatile and precise quantum state engineering by using nonlinear interferometers, *Opt. Express* **27**, 20479 (2019).
- [53] Y. Shaked, Y. Michael, R. Z. Vered, L. Bello, M. Rosenbluh, and A. Pe'er, Lifting the bandwidth limit of optical homodyne measurement with broadband parametric amplification, *Nat. Commun.* **9**, 609 (2018).
- [54] M. Kalash and M. V. Chekhova, Wigner function tomography via optical parametric amplification, *arXiv:2207.10030*.
- [55] A. M. Marino, N. V. Corzo Trejo, and P. D. Lett, Effect of losses on the performance of an Su(1,1) interferometer, *Phys. Rev. A* **86**, 023844 (2012).
- [56] M. Manceau, F. Khalili, and M. Chekhova, Improving the phase super-sensitivity of squeezing-assisted interferometers by squeeze factor unbalancing, *New J. Phys.* **19**, 013014 (2017).
- [57] Y. Liu, J. Li, L. Cui, N. Huo, S. M. Assad, X. Li, and Z. Y. Ou, Loss-tolerant quantum dense metrology with Su(1,1) interferometer, *Opt. Express* **26**, 27705 (2018).
- [58] G. Frascella, S. Agne, F. Y. Khalili, and M. V. Chekhova, Overcoming detection loss and noise in squeezing-based optical sensing, *npj Quantum Inf.* **7**, 72 (2021).
- [59] A. V. Paterova and L. A. Krivitsky, Nonlinear interference in crystal superlattices, *Light* **9**, 82 (2020).
- [60] R. Okamoto, Y. Tokami, and S. Takeuchi, Loss tolerant quantum absorption measurement, *New J. Phys.* **22**, 103016 (2020).
- [61] W. Du, J. Kong, G. Bao, P. Yang, J. Jia, S. Ming, C.-H. Yuan, J. F. Chen, Z. Y. Ou, M. W. Mitchell, and W. Zhang, Su(2)-in-Su(1,1) Nested Interferometer for High Sensitivity, Loss-Tolerant Quantum Metrology, *Phys. Rev. Lett.* **128**, 033601 (2022).
- [62] M. D. C. Pereira, F. E. Becerra, B. L. Glebov, J. Fan, S. W. Nam, and A. Migdall, Demonstrating highly symmetric single-mode, single-photon heralding efficiency in spontaneous parametric downconversion, *Opt. Lett.* **38**, 1609 (2013).
- [63] G. Harder, T. J. Bartley, A. E. Lita, S. W. Nam, T. Gerrits, and C. Silberhorn, Single-Mode Parametric-Down-Conversion States with 50 Photons as a Source for Mesoscopic Quantum Optics, *Phys. Rev. Lett.* **116**, 143601 (2016).
- [64] W. P. Grice, A. B. U'Ren, and I. A. Walmsley, Eliminating frequency and space-time correlations in multiphoton states, *Phys. Rev. A* **64**, 063815 (2001).
- [65] P. J. Mosley, J. S. Lundeen, B. J. Smith, P. Wasylczyk, A. B. U'Ren, C. Silberhorn, and I. A. Walmsley, Heralded

- Generation of Ultrafast Single Photons in Pure Quantum States, *Phys. Rev. Lett.* **100**, 133601 (2008).
- [66] A. Eckstein, A. Christ, P. J. Mosley, and C. Silberhorn, Highly Efficient Single-Pass Source of Pulsed Single-Mode Twin Beams of Light, *Phys. Rev. Lett.* **106**, 013603 (2011).
- [67] See Supplemental Material at <http://link.aps.org/supplemental/10.1103/PhysRevLett.130.203604> for additional details on the model used in this manuscript, intermediated steps in the derivation of the main results, and estimates of realistic absorption cross sections.
- [68] S. Barnett and P. Radmore, *Methods in Theoretical Quantum Optics* (Oxford University Press, New York, 2002).
- [69] P. D. Drummond and Z. Ficek, *Quantum Squeezing* (Springer, Berlin, Heidelberg, 2004).
- [70] C. Gardiner and P. Zoller, *Quantum Noise* (Springer, Berlin, Heidelberg, 2004).
- [71] G. S. Agarwal, Field-correlation effects in multiphoton absorption processes, *Phys. Rev. A* **1**, 1445 (1970).
- [72] M. S. Zubairy and J. J. Yeh, Photon statistics in multiphoton absorption and emission processes, *Phys. Rev. A* **21**, 1624 (1980).
- [73] G. Tóth and I. Apellaniz, Quantum metrology from a quantum information science perspective, *J. Phys. A* **47**, 424006 (2014).
- [74] A. Niezgoda, D. Kajtoch, J. Dziekańska, and E. Witkowska, Optimal quantum interferometry robust to detection noise using spin-1 atomic condensates, *New J. Phys.* **21**, 093037 (2019).
- [75] Even though we cannot completely rule out the possibility of distinct parameters for larger m which give rise to even better resolution, we prove the improved scaling, Eq. (7), for any m in the appendix.
- [76] S. Asban, K. E. Dorfman, and S. Mukamel, Interferometric spectroscopy with quantum light: Revealing out-of-time-ordering correlators, *J. Chem. Phys.* **154**, 210901 (2021).
- [77] S. Asban and S. Mukamel, Distinguishability and which pathway information in multidimensional interferometric spectroscopy with a single entangled photon-pair, *Sci. Adv.* **7**, eabj4566 (2021).
- [78] K. E. Dorfman, S. Asban, B. Gu, and S. Mukamel, Hong-Ou-Mandel interferometry and spectroscopy using entangled photons, *Commun. Phys.* **4**, 49 (2021).
- [79] S. Asban, V. Y. Chernyak, and S. Mukamel, Nonlinear quantum interferometric spectroscopy with entangled photon pairs, *J. Chem. Phys.* **156**, 094202 (2022).
- [80] P.-A. Moreau, E. Toninelli, T. Gregory, and M. J. Padgett, Imaging with quantum states of light, *Nat. Rev. Phys.* **1**, 367 (2019).
- [81] G. B. Lemos, M. Lahiri, S. Ramelow, R. Lapkiewicz, and W. Plick, Quantum imaging and metrology with undetected photons: A tutorial, *J. Opt. Soc. Am.* **39**, 2200 (2022).